The Journal of Veterinary Medical Science

NOTE

Pathology

Necrotizing suppurative nephritis in a Japanese black feedlot steer due to *Proteus mirabilis* infection

Tadatsugu ABE[1)]*, Ayako IIZUKA[1)], Hirokazu KOJIMA[2)], Kumiko KIMURA[3)], Tomoyuki SHIBAHARA[3)] and Makoto HARITANI[3)]

[1)]Tochigi Prefectural Kenou Livestock Hygiene Service Center, 6-8 Hiraidekogyodanchi, Utsunomiya, Tochigi 321-0905, Japan
[2)]Tochigi Prefectural Kenhoku Livestock Hygiene Service Center, 2-12-14 Midori, Nasushiobara, Tochigi 329-2713, Japan
[3)]National Institute of Animal Health, National Agriculture and Food Research Organization, National Research and Development Agency, 3-1-5 Kannondai, Tsukuba, Ibaraki 305-0856, Japan

J. Vet. Med. Sci.
79(4): 709–713, 2017
doi: 10.1292/jvms.15-0636

Received: 4 November 2015
Accepted: 8 February 2017
Published online in J-STAGE: 24 February 2017

ABSTRACT. A Japanese black feedlot steer suddenly died after exhibiting astasia and cramping of the extremities. Necropsy of the animal revealed that the right kidney was enlarged and pale with severe nephrolithiasis. The urinary bladder displayed mucosal hemorrhage. Upon bacteriological investigation, *Proteus mirabilis* was isolated from the liver, spleen, right kidney, lungs and urine. Histopathological examination revealed necrotizing suppurative nephritis with the presence of numerous gram-negative bacilli and fibrinous suppurative cystitis with no bacilli. Immunohistochemical analysis revealed that the bacteria and cytoplasm of the macrophages stained positively with *P. mirabilis* antiserum. Electron microscopy revealed the presence of numerous bacteria in the renal tubules. To our knowledge, this is the first report describing the histopathological aspects of nephritis caused by *P. mirabilis* in cattle.

KEY WORDS: feedlot steer, nephritis, pathology, *Proteus mirabilis*, urolithiasis

The genus *Proteus*, which belongs to the *Enterobacteriaceae* family, comprises gram-negative, motile bacilli that are one of the main pathogens implicated in urinary tract infections [3, 13]. The genus *Proteus* comprises five species: *Proteus hauseri, Proteus mirabilis, Proteus myxofaciens, Proteus penneri* and *Proteus vulgaris* [10]. Although *P. mirabilis* is one of the most common bacteria infecting the urinary tract in humans and dogs [3, 4, 13], no reports to date have described histopathological findings. A recent report regarding urinary infections in cattle caused by *Proteus* did not describe histopathology [14]. Herein, we report a case of nephritis in a feedlot steer in which *P. mirabilis* infection was demonstrated by bacteriological, immunohistochemical and electron microscopic examinations.

A twenty-month-old Japanese black feedlot steer, belonging to a herd of 600 animals, died suddenly after exhibiting astasia and cramping of the extremities that had lasted for an hour on June 19, 2014. The steer had anorexia and claudication of the left hind limb; however, no medical treatment had been administered to the animal.

At necropsy, a large quantity of purple-red urine spouted out when we cut the urethra and there was a strong smell of urine upon cutting the adipose capsule of the right kidney. The right kidney was enlarged, pale with multiple red blotches, and had a rough outer surface. The cut surface displayed diffuse discoloration of the cortex, and many renal (up to 4 cm in diameter) and ureteral calculi (up to 1 cm in diameter) (Fig. 1). In contrast to the right kidney, the outer surface of the left kidney was smooth with some red blotches. The cut surface displayed a few radial lesions. The urinary bladder had severe mucosal hemorrhage and was covered by a thick false membrane (Fig. 2). The serosa adhered to the surrounding adipose tissue. Additionally, accumulation of a large quantity of ascites fluid in the peritoneal cavity and edema of the lungs were observed.

The liver, spleen, right kidney, heart, lungs, brain and urine were cultured on 5% blood agar and deoxycholate hydrogen sulfide lactose agar under aerobic conditions at 37°C for 24 hr. Isolates were subjected to Gram staining and identification by API 20E (bioMérieux, Tokyo, Japan). Gram-negative bacteria with swarming motility on blood agar were isolated from the liver, spleen, right kidney, lungs and urine. The isolates were identified as *P. mirabilis* by API 20E (Profile No. 0736000, 99.9%).

For histopathological examination, the liver, spleen, right kidney, heart, lungs, rumen, reticulum, omasum, abomasum, duodenum to rectum, gallbladder, adrenal glands, bladder, skeletal muscle, brain and jejunal, colic, superficial cervical, subiliac

*Correspondence to: Abe, T., Tochigi Prefectural Kenou Livestock Hygiene Service Center, 6-8 Hiraidekogyodanchi, Utsunomiya, Tochigi 321-0905, Japan.
e-mail: abet07@pref.tochigi.lg.jp

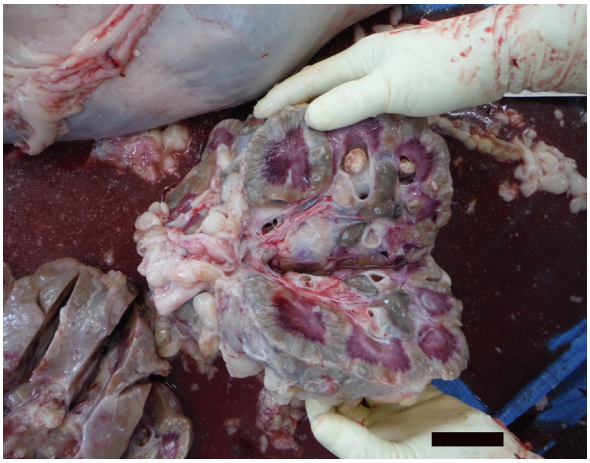

Fig. 1. Gross findings of the right kidney. Diffuse discoloration of the cortex, roughened surface and renal calculi are seen. Bar=5 cm.

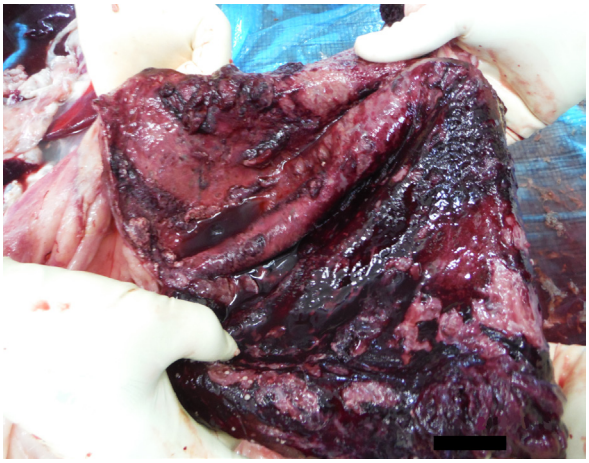

Fig. 2. Gross findings of the urinary bladder. Severe mucosal hemorrhage and a thick false membrane are seen. Bar=5 cm.

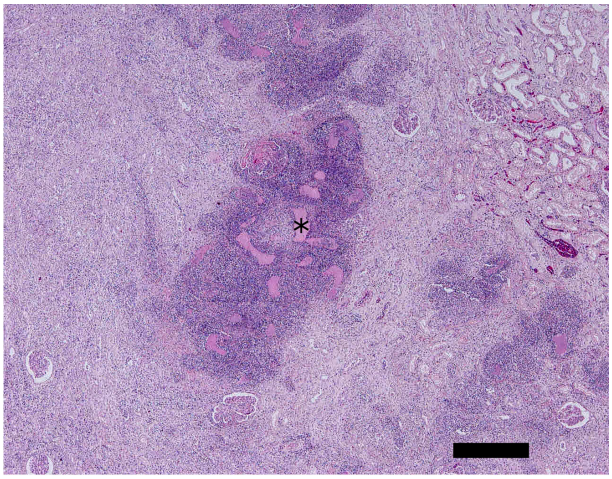

Fig. 3. Histopathological findings of the right kidney. The cortical structure is extensively collapsed, with dense cellular foci including tubular remnants (asterisk). Hematoxylin and eosin. Bar=500 μm.

and superficial inguinal lymph nodes were fixed in 10% neutral buffered formalin, embedded in paraffin wax, sectioned and stained with hematoxylin and eosin. The left kidney was not examined. Additionally, the liver, spleen, right kidney, lungs and bladder sections were subjected to Gram staining. The right kidney was also subjected to Masson's trichrome and periodic acid-methenamine-silver staining (PAM). Histologically, the right kidney showed multifocal, radial or wedge-shaped, necrotizing, suppurative, tubulointerstitial nephritis in the cortex and moderate fibrosis. The cortical structure was extensively collapsed with scattered, dense and cellular foci (Fig. 3). Masson's trichrome-stained sections revealed dissociation of the tubulointerstitial space due to moderate fibrosis (Supplementary Figs. 1 and 2). Additionally, tubular remnants contained numerous gram-negative bacilli, neutrophils and macrophages, surrounded by accumulated neutrophils, macrophages and necrotizing debris (Figs. 4A, 5A and 5B). A few bacteria were seen in the phagocytes (Fig. 5A and 5B). Examination of PAM-stained sections revealed a basement membrane demarcating the tubular remnants (Fig. 4B). Outside the dense, cellular foci, necrotizing tissue was observed with less dense cellular infiltration with moderate fibrosis. Very mild atrophy was observed in glomeruli. Necrosis extended to the outer edge of the outer medulla. As we approached the inner portion of the outer medulla, the infiltrated cells in the tubules predominantly consisted of neutrophils. Structures of the inner medulla and renal pelvis had collapsed due to moderate edema and fibrosis. The structure of the mucous membrane had completely collapsed in the urinary bladder. In the innermost layer, approximately 900-μm thick false membrane consisted of the severe fibrin deposits and mild to moderate neutrophilic infiltration. In the submucosa under the false membrane, multiple hemorrhages, discrete vascular degenerations with thrombosis, moderate edema and laminated

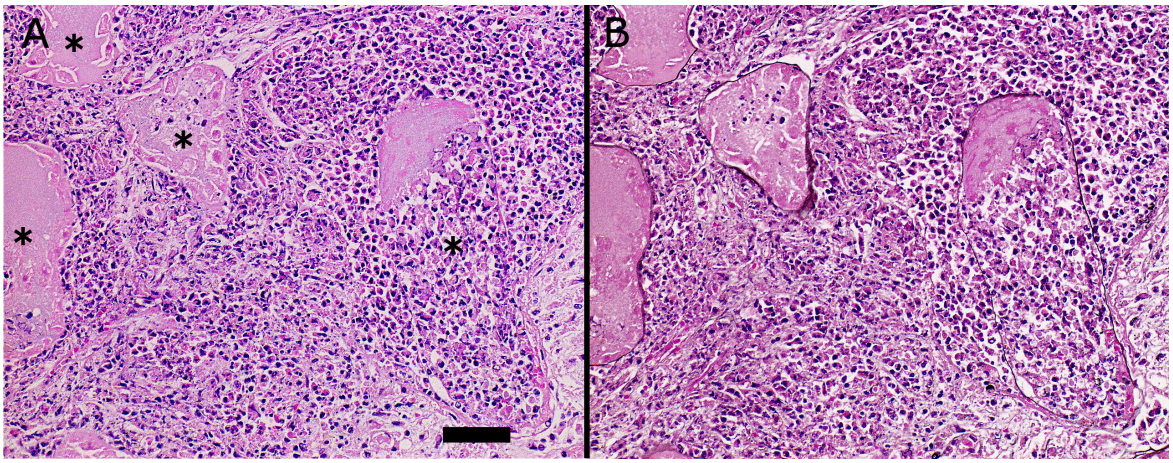

Fig. 4. Histopathological findings of the right kidney. A: Tubular remnants (asterisks) in the lesion contain bacterial colonies, neutrophils and macrophages. The structures are surrounded by a large number of neutrophils and macrophages. Hematoxylin and eosin. B: Basement membranes are observed within each tubular remnant. PAM. Bar=50 μm.

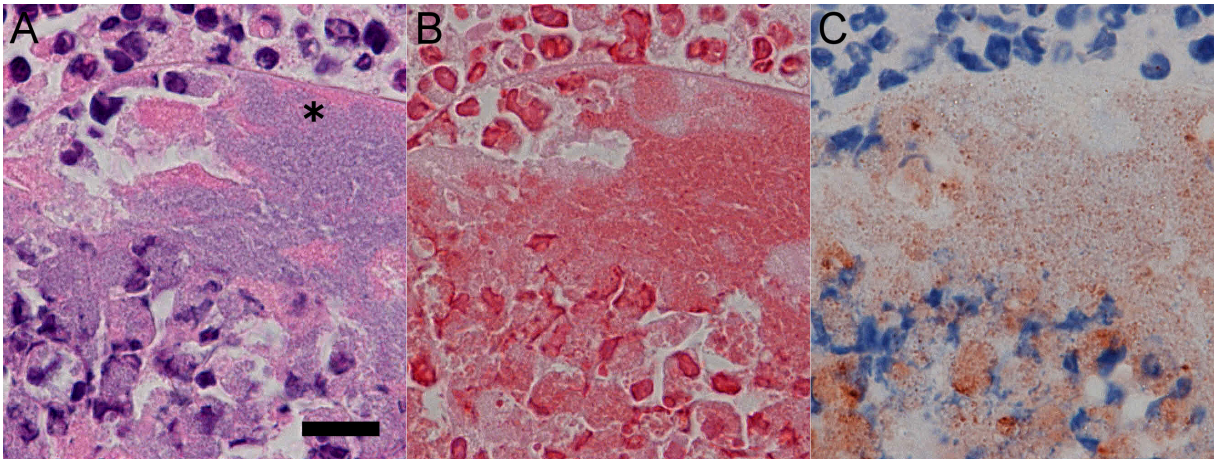

Fig. 5. Histopathological findings of the right kidney. A: Bacterial colonies and macrophages with engulfed bacilli are observed in the tubular remnant (asterisk). H&E. B: Bacteria are found to be gram-negative. C: Bacteria are positively stained by the anti-*P. mirabilis* antibody. Immunohistochemistry. Bar=10 μm.

necrosis with severe neutrophilic infiltration were observed. The muscular layer was thickened with moderate edema, and mild fibroblast hyperplasia and the serous surface demonstrated diffuse fibrinous serositis. Additionally, erythrophagocytosis was often observed in the bleeding areas. Besides the urinary bladder, diffuse fibrinous serositis was also observed in the spleen, intestines and adrenal glands. In the liver, discrete foci of necrosis with mild infiltration of lymphocytes and macrophages, and local collapse of the hepatic tissue were observed. Diffuse severe edema was seen in the lungs. No significant lesions were observed in other tissues except those mentioned here, and no bacterium was observed in other tissues besides the kidney.

Immunohistochemistry was performed using rabbit anti-*P. mirabilis* antiserum (Abcam, Tokyo, Japan) at a dilution of 1:1,024 together with Simple Stain Multi kit and Simple Stain AEC Solution (Nichirei, Tokyo, Japan). Antigen retrieval was performed by immersing sections in 0.01 M citrate buffer (pH 6.0), irradiating them in a microwave oven (preheated to 95°C at 500 W) for 3 cycles of 5 min each. A peace of liver taken from a healthy calf, in which a thick *P. vulgaris or Escherichia coli* suspension was injected, was fixed in 10% neutral buffered formalin and embedded in paraffin wax. Sections cut from the paraffin block served as controls. A positive reaction against anti-*P. mirabilis* antibody was found mainly within tubules in the dense cellular foci. Some phagocytes surrounding the tubules contained a lower number of bacteria and/or antigen (Fig. 5C). A relatively lower extent of positive reaction was observed in the necrotizing tissue with less dense cellular infiltration lying outside the dense cellular areas. Few positive reactions were observed in the false membrane or in the urinary bladder, and no positive reaction was observed in the liver, spleen and lungs. In control tissues, *P. vulgaris* was positively and *E. coli* was negatively stained with the antiserum.

For transmission electron microscopy, renal tissues fixed in 10% neutral buffered formalin were washed with 0.1 M phosphate buffer and post-fixed in phosphate-buffered osmium tetroxide (1%) at 4°C overnight. After dehydrating them, the tissue sections

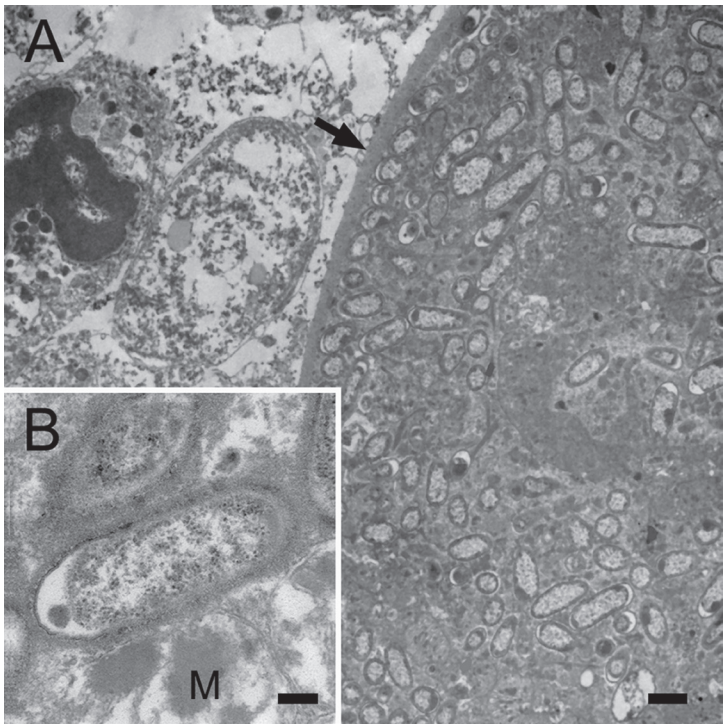

Fig. 6. Transmission electron micrograph of a renal tubule. A: Several rod-shaped bacteria are seen inside the tubule basement membrane (arrow). Bar=2 μm. B: Rod-shaped bacteria show a thin cell wall and dense strands of pili-like, fine filamentous structures on their surface. Bar=200 nm.

were embedded in epoxy resin. Ultrathin sections were then cut, stained with uranyl acetate and lead citrate, and examined by using a transmission electron microscope (H-7500, Hitachi, Tokyo, Japan). A number of rod-shaped bacteria were observed in tubular epithelial cells and macrophages (Fig. 6A). The bacteria were approximately 0.5 μm in diameter and 2 μm in length, and had a thin cell wall that is characteristic of gram-negative bacteria. Surface of some bacteria had dense, stand of pili-like, 8 to 10 nm wide, filamentous structures. No flagellum was seen (Fig. 6B).

For biochemical examination, we measured the quantity of blood urea nitrogen and creatinine in post mortem blood using Fuji DRY-CHEM system (7000Z, Fujifilm, Tokyo, Japan). Blood urea nitrogen and creatinine values were over 140 mg/d*l* and over 24 mg/d*l*, respectively.

In this study, we demonstrated the association between nephritis and *P. mirabilis* infection in a Japanese black feedlot steer using bacteriological, histopathological and electron microscopic examinations. To our knowledge, only one previous report has discussed renal histopathology caused by *P. mirabilis* in mice, wherein histologic changes were observed in the kidneys of mice, seven days post transurethral infection with *P. mirabilis* [1]. The most severe renal lesions in those mice were composed of large cortical necrosis with multiple foci of inflammation and necrosis. These lesions were similar to those in our case. Ultrastructural studies of *P. mirabilis* entry into cells and subsequent bacterial multiplication have been reported using cultured human renal epithelial cells [1, 2]. Bacterial invasion occurs within 30 min of exposure, while at 2 hr, *P. mirabilis* filamentous swarm cells begin to separate and divide into vegetative cells. Finally, within 3 hr, each epithelial cell contains numerous rods throughout the cytoplasm. Similar views were observed in our case by electron microscopy. We isolated *P. mirabilis* from multiple organs. However, as seen in previous reports, we believe that the infection may have ascended to the kidney based on necrotizing suppurative lesions in the nephrons and poor glomerular changes [1, 2].

Lesions of the right kidney are not attributable to *P. mirabilis* infection alone, because gross lesions of the right kidney also resemble chronic nephritis [8]. Additionally, moderate fibrosis was noted, which does not necessarily conform to necrotizing suppurative lesions observed by histopathological examination and the many large renal calculi observed by necropsy. Therefore, it was thought that necrotizing suppurative nephritis due to *P. mirabilis* happened after chronic changes due to renal calculi. Additionally, it was thought that existence of renal calculi induced the ascending infection of *P. mirabilis* [9]. However, the reason for severe cystitis remains unclear due to the low quantity of antigen and absence of bacteria within the lesions.

Proteus species are thought to enhance or induce formation of calculi [5, 6, 11, 12]. Purulent inflammation has been reported to be associated with renal calculi in mice experimentally infected with *P. mirabilis* [7]. In this case, association between *P. mirabilis* and enhancement of renal calculi remains unclear.

To our knowledge, this is the first report describing the histopathological aspects of nephritis caused by *P. mirabilis* in cattle. It is necessary to further examine the pathogenicity of *P. mirabilis* in cattle in future.

REFERENCES

1. Alamuri, P., Eaton, K. A., Himpsl, S. D., Smith, S. N. and Mobley, H. L. 2009. Vaccination with proteus toxic agglutinin, a hemolysin-independent cytotoxin in vivo, protects against *Proteus mirabilis* urinary tract infection. *Infect. Immun.* **77**: 632–641. [Medline] [CrossRef]
2. Chippendale, G. R., Warren, J. W., Trifillis, A. L. and Mobley, H. L. 1994. Internalization of *Proteus mirabilis* by human renal epithelial cells. *Infect. Immun.* **62**: 3115–3121. [Medline]
3. Coker, C., Poore, C. A., Li, X. and Mobley, H. L. T. 2000. Pathogenesis of *Proteus mirabilis* urinary tract infection. *Microbes Infect.* **2**: 1497–1505. [Medline] [CrossRef]
4. Gaastra, W., van Oosterom, R. A., Pieters, E. W., Bergmans, H. E., van Dijk, L., Agnes, A. and ter Huurne, H. M. 1996. Isolation and characterisation of dog uropathogenic Proteus mirabilis strains. *Vet. Microbiol.* **48**: 57–71. [Medline] [CrossRef]
5. Griffith, D. P., Musher, D. M. and Itin, C. 1976. Urease. The primary cause of infection-induced urinary stones. *Invest. Urol.* **13**: 346–350. [Medline]
6. Kramer, G., Klingler, H. C. and Steiner, G. E. 2000. Role of bacteria in the development of kidney stones. *Curr. Opin. Urol.* **10**: 35–38. [Medline] [CrossRef]
7. Li, X., Zhao, H., Lockatell, C. V., Drachenberg, C. B., Johnson, D. E. and Mobley, H. L. 2002. Visualization of *Proteus mirabilis* within the matrix of urease-induced bladder stones during experimental urinary tract infection. *Infect. Immun.* **70**: 389–394. [Medline] [CrossRef]
8. Maxie, M. R. 1993. Pyelonephritis. pp. 511–514. *In*: Pathology of Domestic Animals. 4th ed. (Jubb, K. V. F., Kennedy, P. C. and Palmer N. eds.), Academic Press, San Diego.
9. Newman, S. J. 2012. Pyelonephritis. pp. 635–639. *In*: Pathologic Basis of Veterinary Disease. 5th ed. (Zachary, J. F. and Mcgavin, M. D. eds.), Mosby, St. Louis.
10. Rózalski, A., Sidorczyk, Z. and Kotełko, K. 1997. Potential virulence factors of *Proteus* bacilli. *Microbiol. Mol. Biol. Rev.* **61**: 65–89. [Medline]
11. Torzewska, A. and Różalski, A. 2015. Various intensity of *Proteus mirabilis*-induced crystallization resulting from the changes in the mineral composition of urine. *Acta Biochim. Pol.* **62**: 127–132. [Medline] [CrossRef]
12. Torzewska, A., Staczek, P. and Rózalski, A. 2003. Crystallization of urine mineral components may depend on the chemical nature of Proteus endotoxin polysaccharides. *J. Med. Microbiol.* **52**: 471–477. [Medline] [CrossRef]
13. Warren, J. W. 1996. Clinical presentations and epidemiology of urinary tract infections. pp. 3–27. *In*: Urinary Tract Infection. Molecular Pathogenesis and Clinical Management. (Mobley, H. L. T. and Warren, J. W. eds.), ASM press, Washington, D.C.
14. Yeruham, I., Elad, D., Avidar, Y. and Goshen, T. 2006. A herd level analysis of urinary tract infection in dairy cattle. *Vet. J.* **171**: 172–176. [Medline] [CrossRef]